Earth Syst. Dynam. Discuss., 5, 649–681, 2014
www.earth-syst-dynam-discuss.net/5/649/2014/
doi:10.5194/esdd-5-649-2014

Earth System Dynamics Discussions
Open Access

Global hydrological droughts in the 21st century under a changing hydrological regime

N. Wanders[1], Y. Wada[1], and H. A. J. Van Lanen[2]

[1]Department of Physical Geography, Faculty of Geosciences, Utrecht University, Utrecht, the Netherlands
[2]Hydrology and Quantitative Water Management Group, Centre for Water and Climate, Wageningen University, Wageningen, the Netherlands

Received: 16 May 2014 – Accepted: 19 May 2014 – Published: 6 June 2014

Correspondence to: N. Wanders (n.wanders@uu.nl)

Published by Copernicus Publications on behalf of the European Geosciences Union.

Abstract

Climate change very likely impacts future hydrological drought characteristics across the world. Here, we quantify the impact of climate change on future low flows and associated hydrological drought characteristics on a global scale using an alternative drought identification approach that considers adaptation to future changes in hydrological regime. The global hydrological model PCR-GLOBWB was used to simulate daily discharge at 0.5° globally for 1971–2099. The model was forced with CMIP5 climate projections taken from five GCMs and four emission scenarios (RCPs), from the Inter-Sectoral Impact Model Intercomparison Project.

Drought events occur when discharge is below a threshold. The conventional variable threshold (VTM) was calculated by deriving the threshold from the period 1971–2000. The transient variable threshold (VTM_t) is a non-stationary approach, where the threshold is based on the discharge values of the previous 30 years implying the threshold to vary every year during the 21st century. The VTM_t adjusts to gradual changes in the hydrological regime as response to climate change.

Results show a significant negative trend in the low flow regime over the 21st century for large parts of South America, southern Africa, Australia and the Mediterranean. In 40–52 % of the world reduced low flows are projected, while increased low flows are found in the snow dominated climates.

In 27 % of the global area both the drought duration and the deficit volume are expected to increase when applying the VTM_t. However, this area will significantly increase to 62 % when the VTM is applied. The mean global area in drought, with the VTM_t, remains rather constant (11.7 to 13.4 %), compared to the substantial increase when the VTM is applied (11.7 to 20 %).

The study illustrates that an alternative drought identification that considers adaptation to an altered hydrological regime, has a substantial influence on future hydrological drought characteristics.

ESDD
5, 649–681, 2014

1 Introduction

Drought has large socio-economic and environmental impacts, e.g. on food (rainfed agriculture, irrigation), energy (hydropower, release of cooling water), water-born transport, ecosystem services, wild fires, greenhouse gas emissions (e.g. Wilhite, 2000; Tallaksen and Van Lanen, 2004; Sheffield and Wood, 2011). The 2011 drought in the Horn of Africa caused large famine across the Horn of Africa leaving hundreds of thousands of people in need of assistance and many were regrettable fatalities (United Nations, 2011; Sida et al., 2012). Drought-related heat waves and forest fires caused almost 80 000 death in Europe. Overall losses were estimated to be about 5000 billion Euro over the period 1998–2009 (EEA, 2010). IPCC describes in the Special Report on EXtremes (IPCC-SREX) that droughts will intensify in the 21st century in some seasons and areas (e.g. many European regions, parts of North America, Central America, southern Africa) as result of climate change (Seneviratne et al., 2012). Society needs to be better prepared to ensure future water, food and energy security (e.g. Romm, 2011; Van Vliet et al., 2012; Bourzac, 2013). The severe impacts of large-scale droughts show the need to improve understanding of droughts on continental and global scales, particularly to increase credibility of future drought projections.

Drought is induced by below-normal precipitation or temperature anomalies, which propagate into soil moisture. For management of groundwater and surface water, however, more relevant is the further propagation into hydrological drought (e.g. Van Loon and Van Lanen, 2012). Despite the need for hydrological drought information, most large-scale future drought studies focus either on precipitation or soil moisture (e.g. Burke et al., 2006; Sheffield and Wood, 2008; Sheffield et al., 2012; Dai, 2013; Orlowsky and Seneviratne, 2013; Trenberth et al., 2014). Few studies deal with assessments of large-scale future hydrological drought (e.g. Forzieri et al., 2014a; Wanders and Van Lanen, 2013; Prudhomme et al., 2013). The limitation of these studies are, however, that most of them only use one emission scenario that is based on the previous generation (i.e. CMIP3) of global circulation models (GCMs) and the previous

ESDD
5, 649–681, 2014

scenario projections (i.e. IPCC SRES). Furthermore, Forzieri et al. (2014a) only assesses future drought for one continent (i.e. Europe), rather than spanning the whole globe. An exception is the recent study by Prudhomme et al. (2013), which describes projections of hydrological drought across the world obtained from a comprehensive multi-model ensemble (five GCMs and seven global hydrological models or GHMs) using most recent climate models (CMIP5) and four emission scenarios (i.e. RCPs). All studies on large-scale future hydrological drought, so far, used the so-called threshold method (e.g. Hisdal et al., 2004; Fleig et al., 2006) and drought characteristics in the 21st century are identified by using the threshold of the control or historical period (e.g. 1971–2000). However, one may argue if such stationary approach is suitable for all impact assessments. An updated (transient) threshold for a moving reference period that reflects changes in the hydrological regime over time might be more appropriate to assess such impacts. Vidal et al. (2012) explored the use of a changing drought index for future drought in France. A transient threshold assumes adaptation to long-term changes in the hydrological regime. It is also more in line with the drought definition (Tallaksen and Van Lanen, 2004) being a deviation from normal conditions (i.e. normal implies decadally updated 30 year averages according to the World Meterological Organization guidelines), although the consequences of such statistically-constructed metric for real-world applications need careful investigation (e.g. World Meteorological Organization, 2007; Arguez and Vose, 2010) and should consider if drought-impacted sectors can cope with the changes in the hydrological regime.

The objective of this study is to assess the impact of climate change on future hydrological drought across the globe under a changing hydrological regime, here represented using a transient threshold over the spatially-distributed river discharge. The paper is innovative by using: (i) a gradually-changing, spatially-distributed threshold to adapt to changing hydrological regime, (ii) the latest version of climate models from CMIP5 climate projections, and (iii) the number of emission scenarios: four RCPs (2.6, 4.5, 6.0, 8.5).

ESDD
5, 649–681, 2014

The paper starts with a brief description of the global hydrological model used in this study, forcing data, drought identification approach and the trend analysis, which are followed by the description of the temporal evolution of the spatially-distributed threshold for the river discharge over the 21st century. Next, future drought duration and drought intensity obtained with the transient threshold method, reflecting a changing hydrological regime, are presented and intercompared with the non-transient threshold approach that is derived from the control period (fixed historical period). Results are followed by a discussion that intercompares the outcome of this study with existing assessments of future hydrological drought. It also addresses uncertainty aspects (e.g. variability among GCMs and RCPs), sensitivity of the threshold values applied (Q_{80}, Q_{90}), and the impact of the combined effect of the change in the simulated water availability (hydrological regime) and in the drought characteristics. Eventually, conclusions and recommendation are given.

2 Material and methods

2.1 Model simulation of streamflow

The state-of-the-art global hydrological and water resources model PCR-GLOBWB was used to simulate spatial and temporal continuous fields of discharge and storage in rivers, lakes, and wetlands at a 0.5° spatial resolution (Wada et al., 2010, 2013, 2014; Van Beek et al., 2011). In brief, the model simulates for each grid cell and for each time step (daily) the water storage in two vertically stacked soil layers and an underlying groundwater layer. At the top a canopy with interception storage and a snow cover may be present. Snow accumulation and melt are temperature driven and modelled according to the snow module of the HBV model (Bergström, 1995). To represent rain-snow transition over sub-grid elevation dependent gradients of temperature, 10 elevation zones were distinguished in each grid cell based on the HYDRO1k Elevation Derivative Database, and scaled the 0.5° grid temperate fields with a lapse rate of

0.65 °C per 100 m. The model computes the water exchange between the soil layers, and between the top layer and the atmosphere (rainfall, evaporation and snowmelt). The third layer represents the deeper part of the soil that is exempt from any direct influence of vegetation, and constitutes a groundwater reservoir fed by active recharge. The groundwater store is explicitly parametrized and represented with a linear reservoir model (Kraijenhof van de Leur, 1962). Sub-grid variability is considered by including separately short and tall natural vegetation, open water (lakes, floodplains and wetlands), soil type distribution (FAO Digital Soil Map of the World), and the area fraction of saturated soil calculated by the Improved ARNO scheme (Hagemann and Gates, 2003) as well as the spatio-temporal distribution of groundwater depth based on the groundwater storage and the surface elevations as represented by the 1 km by 1 km Hydro1k data set (https://lta.cr.usgs.gov/HYDRO1K/). Simulated specific runoff from the two soil layers (direct runoff and interflow) and the underlying groundwater layer (base flow) is routed along the river network based on the Simulated Topological Networks (STN30) (Vörösmarty et al., 2000) using the method of characteristic distances (Wada et al., 2014).

The PCR-GLOBWB model and model outputs has been extensively validated in earlier work. Simulated mean, minimum, maximum, and seasonal flow, monthly actual evapotranspiration, and monthly total terrestrial water storage were evaluated against 3600 GRDC observations (http://www.bafg.de/GRDC) ($R^2 \sim 0.9$), the ERA-40 reanalysis data, and the GRACE satellite observations, respectively in earlier work (Van Beek et al., 2011; Wada et al., 2012, 2014), and generally showed good agreement with them. Simulated deficit volumes to derive hydrological drought were also validated against those derived from observed streamflow (from GRDC stations) for major river basins of the world (Wada et al., 2013). The comparison generally showed resonable agreement for most of the basins, which led to the conclusion that PCR-GLOBWB can adequately reproduce low flow conditions and associated drought across the globe.

The model was forced with daily fields of precipitation, reference (potential) evapotranspiration and temperature taken from five global climate models (GCMs; see

ESDD
5, 649–681, 2014
Future hydrological droughts in the 21st century
N. Wanders et al.

Table 1) and four underlying emission scenarios (here accounted for by using four Representative Concentration Pathways or RCPs; see Table 2). The newly available CMIP5 climate projections were obtained through the Inter-Sectoral Impact Model Intercomparison Project (Warszawski et al., 2013). The GCM climate forcing was bias-corrected on a grid-by-grid basis (0.5° grid) by scaling the long-term monthly means of the GCM daily fields to those of the observation-based WATCH climate forcing for the overlapping reference climate 1960–1999 (Hempel et al., 2013). Potential evapotranspiration was calculated with the bias-corrected GCM climate forcing with the method of Hamon (Hamon, 1963). The resulting bias-corrected transient daily climate fields were used to force the model over the period 1971–2099 with a spin-up, reflecting a climate representative prior to the start of the simulation period. The result of each GCM is treated equally and no weight was given to a particular GCM based on the performance against historic climate. As a result, 20 (5 GCMs by 4 RCPs) projections of future daily streamflow were produced.

2.2 Drought calculation

Hydrological drought characteristics (e.g. drought duration and deficit volume) were derived from simulated time series of daily discharge (Q) using the variable threshold level approach (Yevjevich, 1967; Tallaksen et al., 1997; Hisdal et al., 2004). In this study the Q_{90} ($\mathrm{m}^3\,\mathrm{s}^{-1}$) was derived from the flow duration curve, where the Q_{90} is the threshold which is equalled or exceeded for 90 % of the time. This threshold has been selected to study the impact of severe drought conditions and have been used in multiple studies where drought is studied (e.g Fleig et al., 2006; Parry et al., 2010; Wanders and Van Lanen, 2013).

Similar to Wanders and Van Lanen (2013) the drought state is given by:

$$\mathrm{Ds}(t,n) = \begin{cases} 1 & \text{for } Q(t) < Q_x(t,n) \\ 0 & \text{for } Q(t) \geq Q_x(t,n) \end{cases} \quad (1)$$

Discussion Paper | Discussion Paper | Discussion Paper | Discussion Paper |
ESDD
5, 649–681, 2014
Future hydrological droughts in the 21st century
N. Wanders et al.

where $Q_x(t,n)$ is the x percentile threshold $\mathrm{Ds}(t,n)$ is a binary variable indicating if a location or grid cell (n) is in drought at a given time t. The drought duration for each event at n is calculated with:

$$\mathrm{Dur}_{i,n} = \sum_{t=S_i}^{L_i} \mathrm{Ds}(t,n) \qquad (2)$$

where $\mathrm{Dur}_{i,n}$ is the drought duration (d) of event i at n, S_i the first time step of a event i and L_i the last time step of the event. The deficit volume per time step was defined by:

$$\mathrm{Def}(t,n) = \begin{cases} Q_x(t,n) - Q(t,n) & \text{for } \mathrm{Ds}(t,n) = 1 \\ 0 & \text{for } \mathrm{Ds}(t,n) = 0 \end{cases} \qquad (3)$$

where $\mathrm{Def}(t,n)$ is the daily deficit volume of drought i ($\mathrm{m}^3\,\mathrm{s}^{-1}$) at n. The total drought deficit volume for each drought event was calculated with:

$$\mathrm{Def}_i(n) = \sum_{t=S_i}^{L_i} \mathrm{Def}(t,n) \qquad (4)$$

where $\mathrm{Def}_i(n)$ is the total deficit volume of the drought event i ($\mathrm{m}^3\,\mathrm{s}^{-1}$) at n. The deficit volume is the cumulative deviation of the discharge from the threshold over the duration of a drought event. If the $Q_x(t,n)$ equals $0\,\mathrm{m}^3\,\mathrm{s}^{-1}$ by definition a drought will not occur since $\mathrm{Ds}(t,n)$ will remain zero (Eq. 1). If $Q_x(t,n)$ equals $0\,\mathrm{m}^3\,\mathrm{s}^{-1}$ for more than 50 % of the time, no drought characteristics were calculated for this cell. These cells were excluded from the analysis, since frequent zero discharge situations are part of the local climate (i.e. aridity) and are not manifestation of hydrological drought condition or occurrence (Wanders and Van Lanen, 2013).

ESDD
5, 649–681, 2014

The total area in drought (AID) was calculated by:

$$\mathrm{AID}(t) = \frac{\sum_{n=1}^{N} \mathrm{Ds}(t,n)}{N} \quad (5)$$

where AID(t) is the total area in drought at a given time t, N (–) is the total number of cells in the area (e.g. continent, Koeppen–Geiger climate region) or all grid cells (globe) except those arid regions that were excluded from the analysis. The AID(t) can range between 0 and 1, where 0 indicates that there is no cell in the area in drought and 1 indicates that all cells in the area are in drought.

2.3 Variable threshold approach

In this study, two variable threshold approaches were used. The first approach uses the non-transient calculation of the variable threshold level method, where monthly values of Q_x are calculated from simulated discharge over a fixed 30 year period (usually 1971–2000). Thereafter, the monthly values of Q_x are smoothed with a moving average window of 30 days, resulting in the conventional variable threshold (VTM, Van Loon and Van Lanen, 2012; Van Lanen et al., 2013), that was used in the few studies so far on future hydrological drought.

However, present climatology can significantly change over the future period under climate change. This will result in an altered hydrological regime. This could have a significant impact on the detection of drought events, leading to the misrepresentation of drought events as reported by Van Huijgevoort et al. (2014). Areas which become gradually dryer, will be constantly in drought, whereas the opposite will happen in regions with increased low flows. Hydrological regime shifts (e.g earlier snow melt peak) could have a similar impact, where the threshold is not adjusted to the new hydrological conditions. Therefore, we propose the transient variable threshold ($\mathrm{VTM_t}$), where Q_x is based on the discharge values of the previous 30 years (Fig. 1). The monthly values of Q_x are derived from the discharge climatology of the past 30 years instead

ESDD
5, 649–681, 2014
Future hydrological droughts in the 21st century
N. Wanders et al.

of a threshold based on a historic period (1971–2000). Q_x is smoothed with a moving average window of 30 days, resulting in the variable threshold (VTM_t).

The difference between the VTM and VTM_t can be seen in Fig. 1. Both threshold have been applied to the complete time series of river discharges for the period 2000–2099 and drought events were calculated.

2.4 Trend analysis

To study the trends in future drought thresholds, time series of 130 years of river discharges were used. A linear regression was used to study the directionality of the changes and the robustness of those changes. These analyses were performed for each cell separatly to study the effect of regime shifts (e.g due to shifts in snow melt peaks). The robustness in the spatially-distributed trends of the threshold was investigated per season for an ensemble of five GCMs, four RCPs and only statistically significant ($p < 0.05$) were taken into account. For each cell the trend was calculated over the three months belonging to the season for each of the 20 ensemble members. If for a certain season 16 out of 20 ensemble members showed the same trend direction it was assumed to be a robust decrease or increase. If 13 to 15 members had the same direction then the trend is classified as a possible decrease of increase, while for a lower number than 13, no trend was supposed to occur.

Relative trends in drought characteristics were determined by comparing the average drought characteristics for the period 1971–2000 to the period 2070–2099. Per year the number of droughts, number of drought days and total drought deficit were calculated. Yearly statistics were used since drought events often last for more than one month and therefore it would result in large fluctuations in monthly drought statistics. The robustness in the trends in drought characteristics was studied by comparing the outcome from the multiple GCM simulations for each RCP scenario. If for one RCP, all 5 GCMs pointed in the same direction it was assumed to be robust, while if the GCMs showed more discrepancy the changes were deemed not to be robust. This resulted in 3 classes, robust (5 GCMs agree), likely (4 GCMs agree) and plausible (3 GCMs

ESDD
5, 649–681, 2014

agree). The classification was done per grid cell for both the robustness of the trend in average drought duration and the trend in the average deficit volume. These were per grid cell combined in a bivariate classification.

3 Results

3.1 Trends in future low flow regimes

Global trends in the transient variable threshold (VTM_t) were studied for each RCP separately and for the ensemble of five GCMs (Fig. 2). When VTM_t decreases, the long-term low flow regime is reduced in that location and drought characteristics were calculated against the reduced low flows. For the average over all RCP scenarios, 40–52 % of the world will face a decreasing VTM_t for Q_{90}. However, regional variability is large. As expected, RCP2.6 shows the smallest area with a decrease in low flows globally (40 % of the world), while for RCP8.5 the decrease in the threshold is more severe (52 %). Difference in these trends are larger among continents and climate types (see Fig. A1 in Annex for the climate regions used in this study) than among the GCMs; the latter in general show high agreement on the directionality of the change. For the equatorial and warm temperate climate (A and C) the low flows will decrease in 62–77 % of the area, while for the snow and polar climates (D and E) the low flows will increase in 54–90 % of the area (depending on RCP scenario). In these colder regions the increased low flows is mainly due to larger snowmelt and increased precipitation. However, a seasonal shift in low flows was observed for these regions where the snowmelt will occur earlier in the season under a warmer climate. This leads to reduced low flows late in summer, which was observed by the decreasing trend in July to September for most of the Northern Hemisphere (Fig. 2).

Decreasing low flows were observed in: South America, southern Africa, Australia and the Mediterranean area. For the summer months also North America and Europe are largely effected by a decreasing trend. As expected, the decrease in low flows

ESDD
5, 649–681, 2014

is most severe for the highest emission scenario (RCP8.5), while the trends are less obvious for the lowest emission scenario (RCP2.6). However, all RCPs agree on where in the world the low flows will decrease (e.g decrease in variable threshold).

3.2 Comparison in drought characteristics under a non-transient and transient hydrological regime

Drought characteristics, i.e. drought duration and deficit volume, were calculated with the VTM_t for Q_{90} for all RCP scenarios and for all GCMs. Model agreement in the direction of the change is high and distinct patterns are visible in the results (Fig. 3). Globally the agreement between the GCMs is high especially for the snow dominated climate (D), the Mediterranean and South America. We have distinguished four possible cases in the bivariate distribution of the drought duration and the deficit volume: (i) an increase in both drought duration and deficit volume in 27 % of the world (RCP8.5), (ii) increase in duration and decrease in deficit (11 %), (iii) decrease in duration and increase in deficit (17 %), and (iv) a decrease in both drought characteristics (38 %). The remaining part shows no trends of characteristics could not be calculated.

Significant different trends in drought duration and deficit volume were obtained when instead of a gradually-changing hydrological regime (VTM_t) a stationary regime (VTM) was assumed (Figs. 3 and 4). Large parts of the world, especially the Southern Hemisphere show significant increases in both drought duration and deficit volumes. Only the snow affected climates show a decrease in both duration and deficit volume. There is also a higher agreement that the trends in the duration and deficit volume point in the same direction than for VTM_t. An increase in both drought duration and deficit volume is found for 62 % of the world (RCP8.5). The areas covered by the other three cases are: (i) increase in duration and decrease in deficit (4 %), (ii) decrease in duration and increase in deficit (6 %), and (iii) decrease in both drought characteristics (25 %). The differences between Figs. 3 and 4 clearly show that the use of a different threshold approached (VTM_t compared to VTM), which reflect whether a non-stationary or a

ESDD
5, 649–681, 2014

stationary hydrological regime was assumed, have a significant impact on the obtained drought characteristics.

3.3 Trends in drought characteristics under a non-stationary hydrological regime

With the VTM_t for all RCPs in large parts of the snow dominated climate a trend was found towards longer droughts, although the low flows have been increased (Figs. 2 and 3). This is partly due to the decreased length of the snow accumulation season and partly due to the shift in the snowmelt peak. Trends in the deficit volume in these areas are not so pronounced. Precipitation totals for these regions show an increase of 30–100 mm year^{-1} for the period 1971–2000 compared to 2070–2099 (Warszawski et al., 2013). The annual temperature shows an increase of 2–5 °C depending on RCPs when the above-mentioned periods were compared. This confirms the observed earlier snowmelt peak and increased water availability in these regions. The snowmelt peak comes earlier in the year leading to drier soil moisture and groundwater conditions in summer.

For the Mediterranean, the savannah areas of Africa and Middle East, the increase in drought duration is larger for most scenarios (except RCP2.6). The threat is even higher due to the decrease in water availability during low flow conditions (Fig. 2). In these regions water scarcity is a known problem which could be intensified by increased drought durations. The same pattern was found for the interior of Australia, where drought duration is projected to increase and low flows to decrease. However, the impact is less due to lower population density in the region. For these drier areas, temperature rise will be limited to 0.5–3.5 °C, while precipitation will decrease by 35–90 mm year^{-1}.

For South America the decrease in annual precipitation is limited to 12–60 mm year^{-1}, while temperature increase is low (1.2–3.5 °C) compared to global averages (1.5–4.5 °C). However, drought duration in the eastern part of the continent shows a strong increase. In the wetter regions of the Amazon Basin this will likely not cause

ESDD
5, 649–681, 2014

significant impacts. However, the drier regions in Eastern Brazil could be affected as the agricultural areas (mostly irrigation) occrus there.

3.4 Trends in area in drought (AID)

The total area in drought has been calculated for Q_{90} with the transient (VTM_t) and the non-transient (VTM) variable threshold approach. This has been done for the globe and the five Koeppen–Geiger major climate regions. The temporal evolution of the mean and uncertainty of the 20 ensemble members (5 GCMs and 4 RCPs) are given in Fig. 5. The mean global area in drought is projected to slightly increase from 11.7 to 13.4 % under a gradually-changing hydrological regime (VTM_t) (Fig. 5). The uncertainty (one standard deviation) among the members by the end of the 21st century is about 1.9 %. When a stationary hydrological regime was assumed (VTM), then the increase of the global area in drought was substantially larger. The mean area is expected to grow from 11.7 to 19.5 %. The spread among members also is projected to be substantially larger by the end of the 21st century, i.e. 5 % under a stationary hydrological regime.

The area in drought of the tropical (*A*) climate is expected to grow more than the global increase over the 21st century (Fig. 5). The mean area in drought for the tropical climate will slightly increase frome 9.5 to 15.4 % for the non-stationary hydrological regime (VTM_t), whereas it is projected to double (9.5 to 19 %) by the of the century for a stationary hydrological regime (VTM). The spread among the members for the tropical climate is about 2.1 % at the start of the century and is similar for the VTM_t and VTM, but differences in spread are larger by the end of the century when a stationary hydrological regime (VTM_t) was supposed rather than a non-stationary regime (VTM) (3.8 and 6.2 %, respectively).

The difference in area in drought between the VTM_t and VTM approaches among the Koeppen–Geiger major climates is smallest for the snow (*D*) climates (Fig. 5), which is caused by the increased water availability. The mean area in drought is projected to remain constant (around 10.0 %) under a non-stationary hydrological regime (VTM_t), and is expected to only slightly decrease under a stationary regime (VTM) (10.2 to

ESDD
5, 649–681, 2014

6.7 %). Similarly to the other climates, the spread by the end of the 21st century is larger when a stationary hydrological regime was supposed (i.e. 2.6 % for the VTM_t approach and 1.2 % for the VTM_t approach).

4 Discussion

4.1 Intercomparison with existing studies on large-scale future hydrological drought

This study showed that in more than half of the world (about 60 % of the land area) hydrological drought frequency is projected to increase by the end of the 21st century even by considering that the hydrological regime will change. The average drought duration and deficit volume each are expected to increase in around 30 and 40 % of the globe (irrespective of the RCP). Wanders and Van Lanen (2013) report in their global analysis on future hydrological drought using a conceptual hydrological model and 3 GCMs (SRES A2 scenario), a decrease of the number of days in drought pointing at a lower drought frequency and an increase of the average drought duration and deficit volume of the remaining drought events. The characteristics they found cannot directly be compared because these refer to magnitudes rather than to affected areas (this study) and they used another threshold (Q_{80}) and the non-transient variable threshold approach (VTM, i.e. stationary hydrological regime). However, there seems to be some disagreement in at least the drought frequency. Repetition of our drought analysis with Q_{80} and the VTM led to a lower area (40 %) with an increased drought frequency, whereas the area with longer drought events and larger deficit volumes increased by about 50 and 55 %, which indicates agreement in the direction of change of hydrological drought when the same methodology was applied.

Forzieri et al. (2014b) used a large-scale hydrological model and 12 GCMs (SRES A1B scenario) to conclude that low flows in the 2080s are expected to become more extreme in large parts of Europe during the period without frost. Exceptions are

ESDD
5, 649–681, 2014

Scandinavia, the Baltic countries and northern Russia. They used the Q_{80} and the VTM for their analysis. In our study the area in Europe with a higher future drought frequency varied from about 55 % (RCP2.6) to about 75–85 % (other RCPs), which seems to be in line with their study. The area with a higher future average drought deficit volume, however, is about 30–35 % (all RCPs) (see also Fig. 3), which appears to disagree with their conclusion. Repetition of our drought analysis with Q_{80} and the VTM led to a larger area (45–70 %, dependent on RCP) with an increased deficit volume, which agrees more with their outcome.

Prudhomme et al. (2013) explored future hydrological drought using seven global hydrological models (GHMs) and the same GCMs and RCPs as this study. They show that the increase of the global area in drought depends on the RCP, models (GCM, GHM, in particular if the CO_2 effect is included) and the temporal scale (annual, season). The mean increase varies from about 4 % under RCP2.6 to 13 % under RCP8.5. The spread in increase is large with a maximum increase of about 25 %. They used the Q_{90} and the VTM for their analysis. Their results correspond well with our study, but only when using a non-stationary hydrological regime (Fig. 4). Clearly, the increase of global area in hydrological drought is smaller, if the variable threshold is based on a transient hydrological regime (VTM_t).

Intercomparison of future hydrological drought from this study against existing similar studies showed that the outcome points more or less in the same direction, if the same methodology is applied. However, it also shows the large influence of assumptions on projected drought characteristics, such as a transient variable threshold derived from a changing hydrological regime that is introduced in this study vs. the non-transient variable threshold derived from a stationary hydrological regime that has been used in the few existing future hydrological drought studies so far.

Van Huijgevoort et al. (2014) describe that it is not straightforward to determine future hydrological drought with the VTM derived from observations in the past. This can lead to unintended future drought events (short-lived, very high deficit volume) for climates and hydrological systems with a sharp rise in the hydrograph (e.g. cold climates with

ESDD
5, 649–681, 2014

pronounced snow melt, monsoon climates) that will face a regime shift. The VTM_t method proposed in this study implicitly handles this impact of a regime shift.

When the transient threshold decreases (Fig. 2) it implies that the low flows are reduced in that location. When these reduced low flows coincide with an increase in drought duration and deficit volume this will have a large impact on the water availability under drought (15 % of the world). This poses enormous challenges to society and nature to adapt, especially in developing countries, which usually are very vulnerable.

4.2 Uncertainty

Differences between projected temperature and precipitation with GCMs and RCPs used (Tables 1 and 2) are large (e.g. Warszawski et al., 2013). Clearly, these differences influence future hydrological drought, as illustrated by Prudhomme et al. (2013) and Wanders and Van Lanen (2013). The spread in the projected temporal evolution of the global area in hydrological drought, as shown in Fig. 5, also illustrates the impact of different climate drivers. In particular, the spread is large for the Tropical climate and Desert climate. Prudhomme et al. (2013) conclude that the model structure of the hydrological models substantially contributes to uncertainty in future hydrological drought, particularly if the rather hard predictable response of plants to a changing CO_2 concentration (i.e. CO_2 effect) is implemented. The PCR-GLOBWB model used in this study, is one of the seven hydrological models that contributed to the ISI-MIP project (Warszawski et al., 2013); the CO_2 effect is not included. The model has proven to reasonably capture hydrological characteristics (Wada et al., 2013).

Another source of uncertainty is the drought identification methodology that should be defined by the drought-impacted sectors. These sectors determine the magnitude of the threshold level to be used (e.g. Q_{80} instead of Q_{90}) and whether a fixed threshold (constant through the whole period) or a variable threshold method should be applied. Similarly, these sectors determine if a VTM_t for the variable threshold approach, should be chosen for the assessment of future drought that considers a gradually changing hydrological regime in the future or that a VTM should be taken that is based on a

ESDD
5, 649–681, 2014
Future hydrological droughts in the 21st century
N. Wanders et al.

stationary hydrological regime derived from historical observations. Table 3 shows that the global area with increased average hydrological drought duration is hardly affected by the selection of the magnitude of the threshold level (maximum difference in % change is 1 %). Differences for the average deficit volume are slightly larger (maximum difference in % change of global area with increased deficit volume is 4 %). Differences are substantially larger whether the VTM_t or the VTM was applied. The difference in change of area in hydrological drought with increased drought duration is 13 % for RCP2.6 and 18–19 % for the other RCPs. The difference in change for the drought deficit volume is 9 % for RCP2.6, 13 % for RCP4.5 and 6.0, and 17 % for RCP8.5. As expected, it appears that the difference in projected change of global area in hydrological drought between the two variable threshold methods is larger for the more extreme RCPs.

5 Conclusions

In this study future hydrological drought that considers adaptation to a gradually-changing hydrological regime has been studied. An ensemble of 5 General Circulation Models (GMCs) and 4 Representative Climate Pathways (RCPs) has been used as meteorological forcing for the global hydrological model PCR-GLOBWB. Daily discharge has been simulated for the period 1971–2099 and drought in discharge was detected using two threshold level approaches. The conventionally applied variable threshold (VTM) was calculated by deriving the threshold from the period 1971–2000 and subsequently the VTM was used for the period 2000–2099 to identify future drought characteristics (stationary approach). As an alternative, the transient variable threshold (VTM_t) was proposed, which is based on the discharge values of the previous 30 years, where the threshold will vary over time (non-stationary approach). The VTM_t reflects changes in the hydrological regime as response to climate change. The VTM_t is supposed to provide more realistic future hydrological drought characteristics when the impacted sectors are able to adapt to gradual changes in the hydrological regime. The

ESDD
5, 649–681, 2014
Future hydrological droughts in the 21st century
N. Wanders et al.

Q_{90} (discharge that is equalled or exceeded 90 % of the time) has been used both for the VTM and $\mathrm{VTM_t}$.

Result based on the $\mathrm{VTM_t}$ show that low flows are projected to become lower in 40–52 % of the world (dependent on the RCP). In the equatorial and warm temperate (A and C) climates the low flows will decrease in 62–77 % of the area, while for the snow and polar (D and E) climates the low flows will decrease in 10–46 % of the area. The small decrease in low flows for the snow affected climates is mainly due to increased precipitation leading to higher low flows. A regime shift was also found, where snow melt will occur earlier in the season due to higher temperatures leading to drier conditions during the summer. Droughts were identified relative to these altered low flow conditions when applying the $\mathrm{VTM_t}$.

Future hydrological drought characteristics strongly depend on whether the impact of adaptation to a gradually changing hydrological regime due to climate change is considered ($\mathrm{VTM_t}$) or not (VTM). The global area with an increase of both duration and deficit volume is only 27 % (RCP8.5) by the end of the 21st century by using the $\mathrm{VTM_t}$, whereas this is substantially larger (62 %) when the VTM is applied. The area with a decrease of both the duration and the deficit volume is larger when the $\mathrm{VTM_t}$ was used rather than the VTM (38 and 25 %, respectively). The global area in drought is also strongly affected by whether the $\mathrm{VTM_t}$ or VTM is applied. The mean global area with drought in discharge is projected to increase by only a few per cent (11.7 to 13.4 %) when using the $\mathrm{VTM_t}$, but it is expected to become about 20 % (RCP8.5) when the stationary approach was applied (VTM). The spread in projected areal increase among ensemble members also is substantially smaller when the $\mathrm{VTM_t}$ is used instead of the VTM.

Results show that although the $\mathrm{VTM_t}$ has been used, drought duration and deficit volume is expected to increase in large parts of South America, southern Africa and the Mediterranean. In 15 % of the world a negative trend in low flows is found in combination with an increase in drought duration and deficit volume, which points at a likelihood of severe future water stress.

ESDD
5, 649–681, 2014

The study demonstrates that an alternative way to identify hydrological drought that considers adaptation to an altered hydrological regime caused by climate change, has a significant influence on future hydrological drought characteristics. For sectors that can deal with gradual changes in the hydrological regime the transient variable threshold (VTM_t) is an alternative approach to calculate drought characteristics.

Acknowledgements. NW was funded by a grant from the user support program Space Research of NWO (contract number NWO GO-AO/30). This work has been supported by the framework of ISI-MIP funded by the German Federal Ministry of Education and Research (BMBF) (Projectfunding reference number: 01LS1201A). This research was undertaken as part of the European Union FP7 Collaborative project DROUGHT-R&SPI (grant 282769, HvL). The research is part of the programme of the Wageningen Institute for Environment and Climate Research (WIMEK-SENSE), and it supports the work of the UNESCO-IHP VII FRIEND-Water programme (HvL).

References

Arguez, A. and Vose, R. S.: The definition of the standard WMO climate normal: the key to deriving alternative climate normals, B. Am. Meteorol. Soc., 92, 699–704, doi:10.1175/2010BAMS2955.1, 2010. 652

Bergström, S.: The HBV model, in: Computer Models of Watershed Hydrology, edited by: Singh, V. P., Water Resour. Publ., Highlands Ranch, Colorado, USA, 443–476, 1995. 653

Bourzac, K.: Water: the flow of technology, Nature, 501, S4–S6, doi:10.1038/501S4a, 2013. 651

Burke, E. J., Brown, S. J., and Christidis, N.: Modeling the recent evolution of global drought and projections for the twenty-first century with the Hadley Centre Climate Model, J. Hydrometeorol., 7, 1113–1125, doi:10.1175/JHM544.1, 2006. 651

Dai, A.: Increasing drought under global warming in observations and models, Nat. Clim. Change, 3, 52–58, 2013. 651

EEA: Mapping the impact of Natural Hazards and technological accidents in Europe, An overview of the last decade, Tech. Rep. 13/2010, EEA, Copenhagen, 2010. 651

ESDD
5, 649–681, 2014

Fleig, A. K., Tallaksen, L. M., Hisdal, H., and Demuth, S.: A global evaluation of streamflow drought characteristics, Hydrol. Earth Syst. Sci., 10, 535–552, doi:10.5194/hess-10-535-2006, 2006. 652, 655

Forzieri, G., Feyen, L., Rojas, R., Flörke, M., Wimmer, F., and Bianchi, A.: Ensemble projections of future streamflow droughts in Europe, Hydrol. Earth Syst. Sci., 18, 85–108, doi:10.5194/hess-18-85-2014, 2014a. 651, 652

Forzieri, G., Feyen, L., Rojas, R., Flörke, M., Wimmer, F., and Bianchi, A.: Ensemble projections of future streamflow droughts in Europe, Hydrol. Earth Syst. Sci., 18, 85–108, doi:10.5194/hess-18-85-2014, 2014b. 663

Hagemann, S. and Gates, L. D.: Improving a sub-grid runoff parameterization scheme for climate models by the use of high resolution data derived from satellite observations, Clim. Dynam., 21, 349–359, doi:10.1007/s00382-003-0349-x, 2003. 654

Hamon, W. R.: Computation of direct runoff amounts from storm rainfall, Int. Assoc. Sci. Hydrol. Publ., 63, 52–62, 1963. 655

Hempel, S., Frieler, K., Warszawski, L., Schewe, J., and Piontek, F.: A trend-preserving bias correction – the ISI-MIP approach, Earth Syst. Dynam., 4, 219–236, doi:10.5194/esd-4-219-2013, 2013. 655

Hisdal, H., Tallaksen, L., Clausen, B., Peters, E., and Gustard, A.: Hydrological drought characteristics, in: Hydrological Drought: Processes and Estimation Methods for Streamflow and Groundwater, edited by: Tallaksen, L. and Lanen, H., no. 48 in Development in Water Science, Elsevier, Amsterdam, the Netherlands, 139–198, 2004. 652, 655

Kraijenhof van de Leur, D.: Some effects of the unsaturated zone on nonsteady free-surface groundwater flow as studied in a sealed granular model, J. Geophys. Res., 67, 4347–4362, 1962. 654

Orlowsky, B. and Seneviratne, S. I.: Elusive drought: uncertainty in observed trends and short- and long-term CMIP5 projections, Hydrol. Earth Syst. Sci., 17, 1765–1781, doi:10.5194/hess-17-1765-2013, 2013. 651

Parry, S., Prudhomme, C., Hannaford, J., and Lloyd-Hughes, B.: Examining the spatio-temporal evolution and characteristics of large-scale European droughts, in: Role of Hydrology in Managing Consequences of a Changing Global Environment, Proceedings of the BHS Third International Symposium, edited by: Kirby, C., British Hydrological Society, Newcastle, 135–142, 2010. 655

ESDD
5, 649–681, 2014

Prudhomme, C., Giuntoli, I., Robinson, E. L., Clark, D. B., Arnell, N. W., Dankers, R., Fekete, B. M., Franssen, W., Gerten, D., Gosling, S. N., Hagemann, S., Hannah, D. M., Kim, H., Masaki, Y., Satoh, Y., Stacke, T., Wada, Y., and Wisser, D.: Hydrological droughts in the 21st century, hotspots and uncertainties from a global multimodel ensemble experiment, P. Natl. Acad. Sci. USA, doi:10.1073/pnas.1222473110, in press, 2013. 651, 652, 664, 665

Romm, J.: Desertification: the next dust bowl, Nature, 478, 450–451, doi:10.1038/478450a, 2011. 651

Seneviratne, S. I., Nicholls, N., Easterling, D., Goodess, C. M., Kanae, S., Kossin, J., Luo, Y., Marengo, J., McInnes, K., Rahimi, M., Reichstein, M., Sorteberg, A., Vera, C., and Zhang, X.: Changes in climate extremes and their impacts on the natural physical environment, in: A Special Report of Working Groups I and II of the Intergovernmental Panel on Climate Change (IPCC), Cambridge University Press, Cambridge, UK, New York, NY, USA, 109–230, 2012. 651

Sheffield, J. and Wood, E.: Projected changes in drought occurrence under future global warming from multi-model, multi-scenario, IPCC AR4 simulations, Clim. Dynam., 31, 79–105, doi:10.1007/s00382-007-0340-z, 2008. 651

Sheffield, J. and Wood, E. F.: Drought: Past Problems and Future Scenarios, Earthscan, London, 2011. 651

Sheffield, J., Wood, E. F., and Roderick, M. L.: Little change in global drought over the past 60 years, Nature, 491, 435–438, doi:10.1038/nature11575, 2012. 651

Sida, L., Gray, B., and Asmare, E.: Real-time evaluation of the humanitarian response to the Horn of African drought crises, Tech. rep., Inter-Agency Standing Committee, Amsterdam, the Netherlands, 2012. 651

Tallaksen, L. and Van Lanen, H.: Hydrological Drought: Processes and Estimation Methods for Streamflow and Groundwater, no. 48 in Development in water science, Elsevier, Geneva, Switzerland, 2004. 651, 652

Tallaksen, L., Madsen, H., and Clausen, B.: On the definition and modelling of streamflow drought duration and deficit volume, Hydrolog. Sci. J., 42, 15–33, 1997. 655

Trenberth, K. E., Dai, A., van der Schrier, G., Jones, P. D., Barichivich, J., Briffa, K. R., and Sheffield, J.: Global warming and changes in drought, Nat. Clim. Change, 4, 17–22, doi:10.1038/nclimate2067, 2014. 651

United Nations: Humanitarian Requirements for the Horn of Africa Drought 2011, Tech. rep., Office for the Coordination of Humanitarian Affairs (OCHA), New York, Geneva, 2011. 651

ESDD
5, 649–681, 2014

Van Beek, L. P. H., Wada, Y., and Bierkens, M. F. P.: Global monthly water stress: I. Water balance and water availability, Water Resour. Res., 47, W07517, doi:10.1029/2010WR009791, 2011. 653, 654

Van Huijgevoort, M., Van Lanen, H., Teuling, A., and Uijlenhoet, R.: Identification of changes in hydrological drought characteristics from a multi-GCM driven ensemble constrained with observed discharge, J. Hydrol., 512, 421–434, 2014. 657, 664

Van Lanen, H. A. J., Wanders, N., Tallaksen, L. M., and Van Loon, A. F.: Hydrological drought across the world: impact of climate and physical catchment structure, Hydrol. Earth Syst. Sci., 17, 1715–1732, doi:10.5194/hess-17-1715-2013, 2013. 657

Van Loon, A. F. and Van Lanen, H. A. J.: A process-based typology of hydrological drought, Hydrol. Earth Syst. Sci., 16, 1915–1946, doi:10.5194/hess-16-1915-2012, 2012. 651, 657

Van Vliet, M. T. H., Yearsley, J. R., Ludwig, F., Vogele, S., Lettenmaier, D. P., and Kabat, P.: Vulnerability of US and European electricity supply to climate change, Nat. Clim. Change, 2, 676–681, doi:10.1038/nclimate1546, 2012. 651

Van Vuuren, P., Edmonds, J., Kainuma, M., Riahi, K., Thomson, A., Hibbard, K., Hurtt, G., Kram, T., Krey, V., Lamarque, J.-F., Masui, T., Meinshausen, M., Nakicenovic, N., Smith, S., and Rose, S.: The representative concentration pathways: an overview, Climatic Change, 109, 5–31, doi:10.1007/s10584-011-0148-z, 2011. 674

Vidal, J.-P., Martin, E., Kitova, N., Najac, J., and Soubeyroux, J.-M.: Evolution of spatio-temporal drought characteristics: validation, projections and effect of adaptation scenarios, Hydrol. Earth Syst. Sci., 16, 2935–2955, doi:10.5194/hess-16-2935-2012, 2012. 652

Vörösmarty, C. J., Fekete, B. M., Meybeck, M., and Lammers, R. B.: A simulated topological network representing the global system of rivers at 30-minute spatial resolution (STN-30), Global Biogeochem. Cy., 14, 599–621, 2000. 654

Wada, Y., van Beek, L. P. H., van Kempen, C. M., Reckman, J. W. T. M., Vasak, S., and Bierkens, M. F. P.: Global depletion of groundwater resources, Geophys. Res. Lett., 37, L20402, doi:10.1029/2010GL044571, 2010. 653

Wada, Y., van Beek, L. P. H., and Bierkens, M. F. P.: Nonsustainable groundwater sustaining irrigation: a global assessment, Water Resour. Res., 48, W00L06, doi:10.1029/2011WR010562, 2012. 654

Wada, Y., van Beek, L. P. H., Wanders, N., and Bierkens, M. F. P.: Human water consumption intensifies hydrological drought worldwide, Environ. Res. Lett., 8, 034036, doi:10.1088/1748-9326/8/3/034036, 2013. 653, 654, 665

ESDD
5, 649–681, 2014
Future hydrological droughts in the 21st century
N. Wanders et al.

Wada, Y., Wisser, D., and Bierkens, M. F. P.: Global modeling of withdrawal, allocation and consumptive use of surface water and groundwater resources, Earth Syst. Dynam., 5, 15–40, doi:10.5194/esd-5-15-2014, 2014. 653, 654

Wanders, N. and van Lanen, H. A. J.: Future discharge drought across climate regions around the world modelled with a synthetic hydrological modelling approach forced by three General Circulation Models, Nat. Hazards Earth Syst. Sci. Discuss., 1, 7701–7738, doi:10.5194/nhessd-1-7701-2013, 2013. 651, 655, 656, 663, 665

Warszawski, L., Frieler, K., Huber, V., Piontek, F., Serdeczny, O., and Schewe, J.: The Inter-Sectoral Impact Model Intercomparison Project (ISI-MIP): project framework, P. Natl. Acad. Sci. USA, 111, 3228–3232, doi:10.1073/pnas.1312330110, 2013. 655, 661, 665

Wilhite, D.: Drought: A Global Assessment, Routledge, New York, 2000. 651

World Meteorological Organization: The Role of Climatological Normals in a Changing Climate, wCDMP-No. 61, WMO-TD/No. 1377, Geneva, 2007. 652

Yevjevich, V.: An objective approach to definition and investigation of continental hydrological droughts, Hydrology papers 23, Colorado state university, Fort Collins, USA, 1967. 655

ESDD
5, 649–681, 2014

Future hydrological droughts in the 21st century

N. Wanders et al.

Table 1. GCMs (Global Climate Models) used in this study.

GCM	Organization
HadGEM2-ES	Met Office Hadley Centre
IPSL-CM5A-LR	Institute Pierre-Simon Laplace
MIROC-ESM-CHEM	JAMSTEC, NIES, AORI (The University of Tokyo)
GFDL-ESM2M	NOAA Geophysical Fluid Dynamics Laboratory
NorESM1-M	Norwegian Climate Centre

ESDD
5, 649–681, 2014

Table 2. Overview of representative concentration pathways (RCPs) (Van Vuuren et al., 2011). Radiative forcing values include the net effect of all anthropogenic greenhouse gases and other forcing agents.

RCP	Scenario
2.6	Peak in radiative forcing at ~ 3.1 $W m^2$ (~ 490 ppm CO_2 equivalent) before 2100 and then decline (the selected pathway declines to 2.6 $W m^2$ by 2100)
4.5	Stabilization without overshoot pathway to 4.5 $W m^2$ (~ 650 ppm CO_2 equivalent) at stabilization after 2100
6.0	Stabilization without overshoot pathway to 6 $W m^2$ (~ 850 ppm CO_2 equivalent) at stabilization after 2100
8.5	Rising radiative forcing pathway leading to 8.5 $W m^2$ (~ 1370 ppm CO_2 equivalent) by 2100

ESDD
5, 649–681, 2014

Table 3. Change in global area (%) with increased hydrological drought duration and drought deficit volume: % change derived from 30 year averages of future (2070–2099) against reference (1971–2000) for two variable threshold methods (VTM_t and VTM) and two thresholds Q_{80} and Q_{90}.

Drougth identification method	RCP	% of world with			
		Increased drought duration		Increased drought deficit	
		Q_{80}	Q_{90}	Q_{80}	Q_{90}
Transient (VTM_t)	2.6	33	33	42	38
	4.5	32	32	41	38
	6.0	35	34	43	40
	8.5	33	33	40	39
Non-transient (VTM)	2.6		46		47
	4.5		50		51
	6.0		52		53
	8.5		54		56

ESDD
5, 649–681, 2014
Future hydrological droughts in the 21st century
N. Wanders et al.

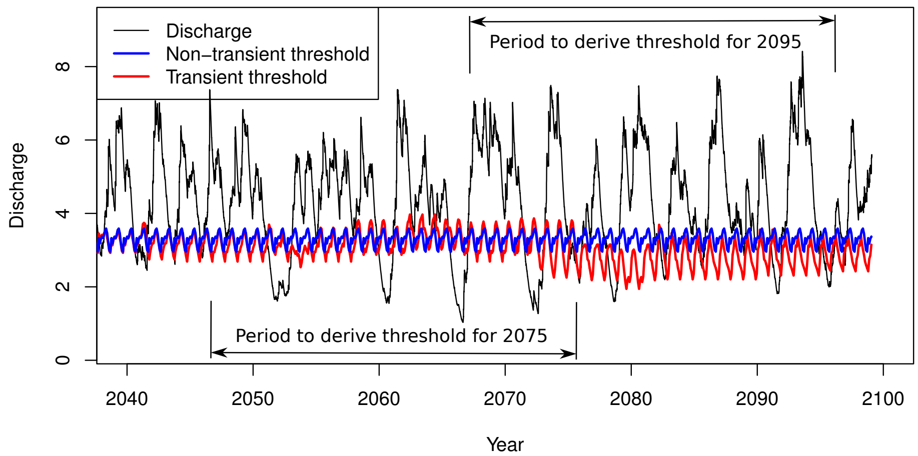

Figure 1. Example time series with schematic overview of the non-stationary variable threshold (VTM), which is constant over the 21st century, and the stationary variable threshold (VTM_t) that considers the gradually-changing future hydrological regime.

ESDD
5, 649–681, 2014

Future hydrological droughts in the 21st century

N. Wanders et al.

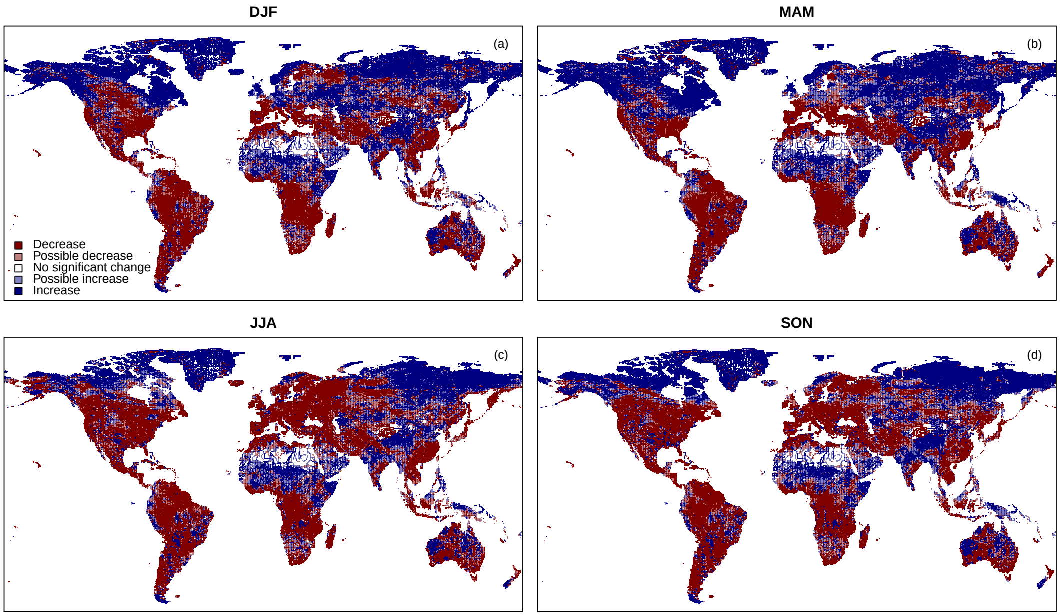

Figure 2. Average trends in the transient Q_{90} threshold in the four seasons derived from simulation with PCR-GLOBWB. Trends are aggregated over 3 month periods for an ensemble of 20 members consisting of 4 RCPs and 5 GCMs. An increase or decrease is significant when over 16 ensemble members show similar trends. When over 13 ensemble members agree on the directionality of the change, the trend is deemed possible.

ESDD
5, 649–681, 2014

Title Page
Abstract | Introduction
Conclusions | References
Tables | Figures
◂ | ▸
Back | Close
Full Screen / Esc
Printer-friendly Version
Interactive Discussion

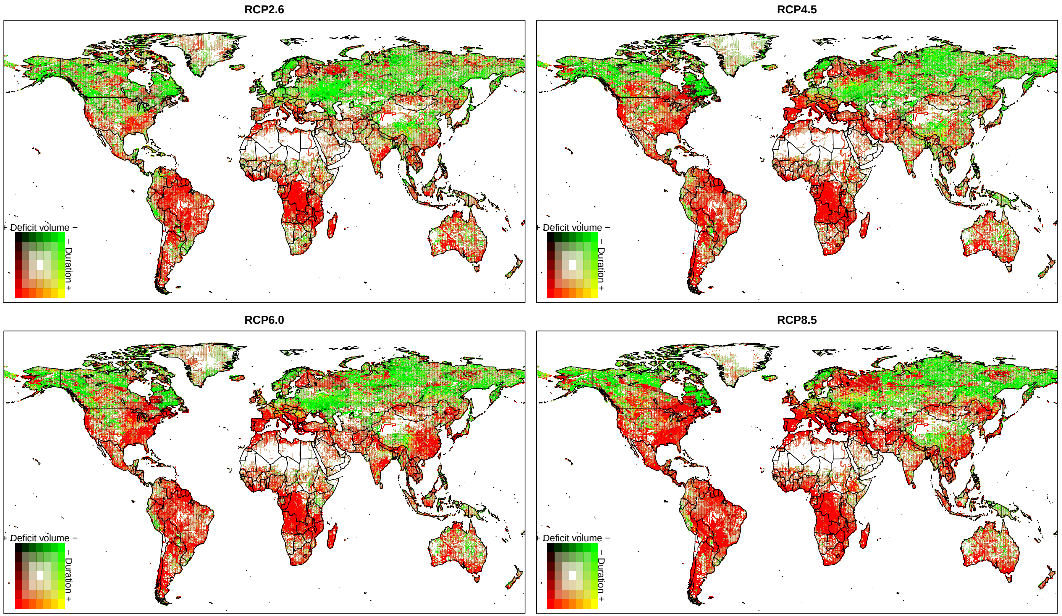

Figure 3. Average trends in drought duration and drought deficit volume, derived with a transient Q_{90} threshold from discharge simulation of PCR-GLOBWB. Maps indicate the changes per RCP for a ensemble of 5 GCMs. Colors indicate the robustness of the trend where the darkest colors are robust (5 GCMs agree), thereafter likely (4 GCMs agree) and plausible (3 GCMs agree). A white color indicates areas where no drought characteristics were calculated.

ESDD
5, 649–681, 2014

Future hydrological droughts in the 21st century

N. Wanders et al.

ESDD
5, 649–681, 2014

Future hydrological droughts in the 21st century

N. Wanders et al.

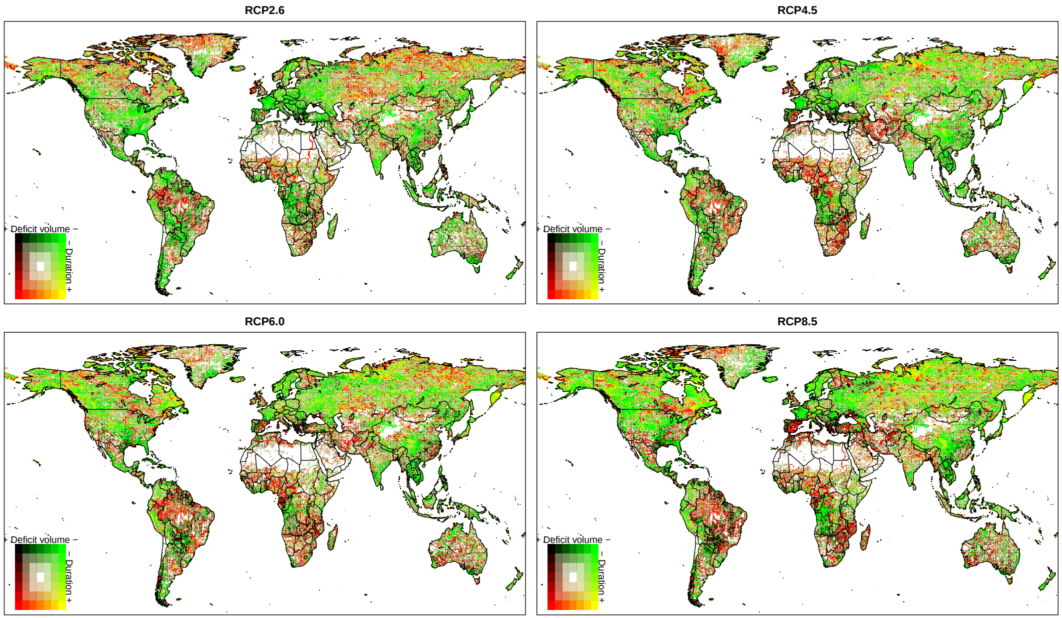

Figure 4. Average trends in drought duration and drought deficit volume, derived with the non-transient Q_{90} threshold from discharge simulation of PCR-GLOBWB. Maps indicate the changes per RCP for a ensemble of 5 GCMs. Colors indicate the robustness of the trend where the darkest colors are robust (5 GCMs agree), thereafter likely (4 GCMs agree) and plausible (3 GCMs agree). A white color indicates areas where no drought characteristics were calculated.

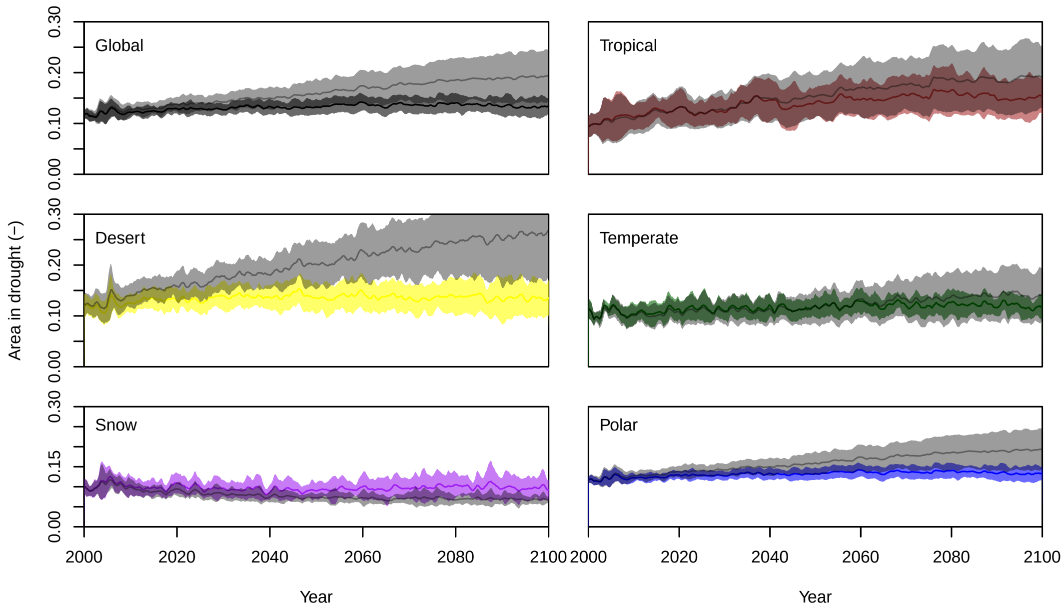

Figure 5. Projected evolution of ensemble mean area (solid line) and the spread in hydrological drought in the 21st century derived from simulation with PCR-GLOBWB, forced by an ensemble of 20 scenarios consisting of four RCPs and five GCMs. The evolution is given for the globe and for the five major Koeppen–Geiger climatic regions. The coloured lines present the evolution under a changing hydrological regime (transient variable threshold, VTM_t) and black/gray the evolution under a stationary hydrological regime (non-transient variable threshold, VTM).

ESDD
5, 649–681, 2014

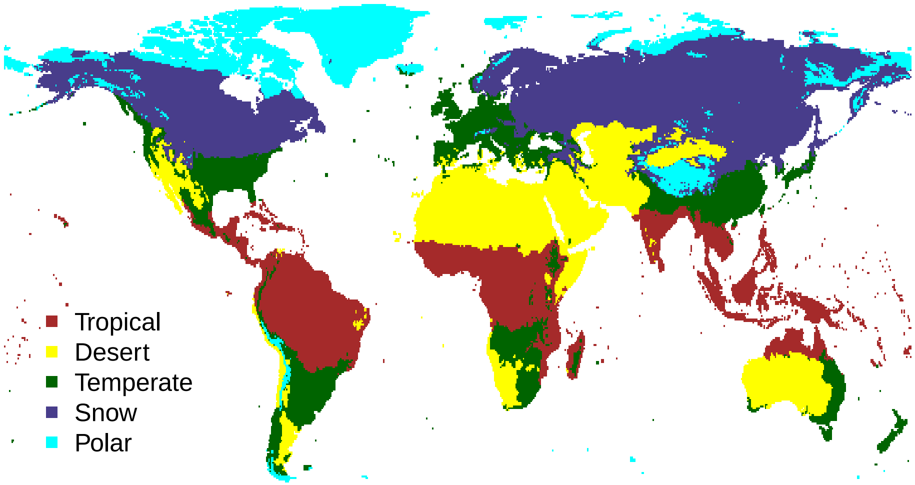

Figure A1. Global map of Köppen–Geiger climate types.

ESDD
5, 649–681, 2014